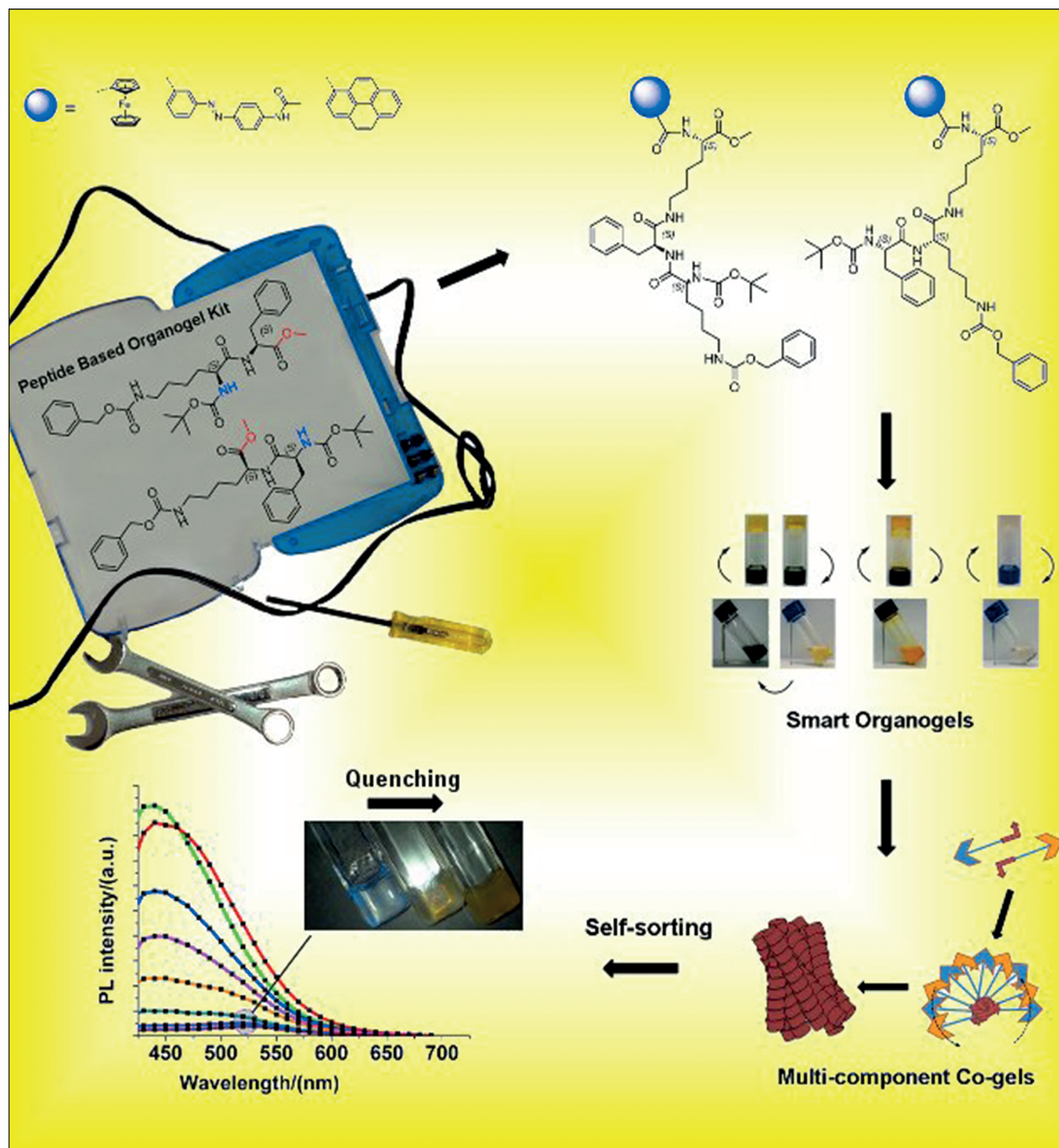


Small-Peptide-Based Organogel Kit: Towards the Development of Multicomponent Self-Sorting Organogels

Rouzbeh Afrasiabi and Heinz-Bernhard Kraatz*^[a]



Abstract: The results presented here highlight the extremely useful nature of ultra-short peptides as building blocks in the development of smart multicomponent supramolecular devices. A facile bottom-up strategy for the synthesis of a small library of stimuli-responsive smart organogelators has been proposed based on the predictive self-assembly of ultra-short peptides. More importantly, the narcissistic self-sorting of the gelators has been evalu-

ated as a simple method for the efficient co-assembly of a donor-acceptor dual-component gel, allowing the investigation of possible future applications of similar systems in the development of a supramolecular photo-conversion device. Interestingly, it was ob-

Keywords: gels • nanomaterials • peptides • self-assembly • UV/Vis spectroscopy

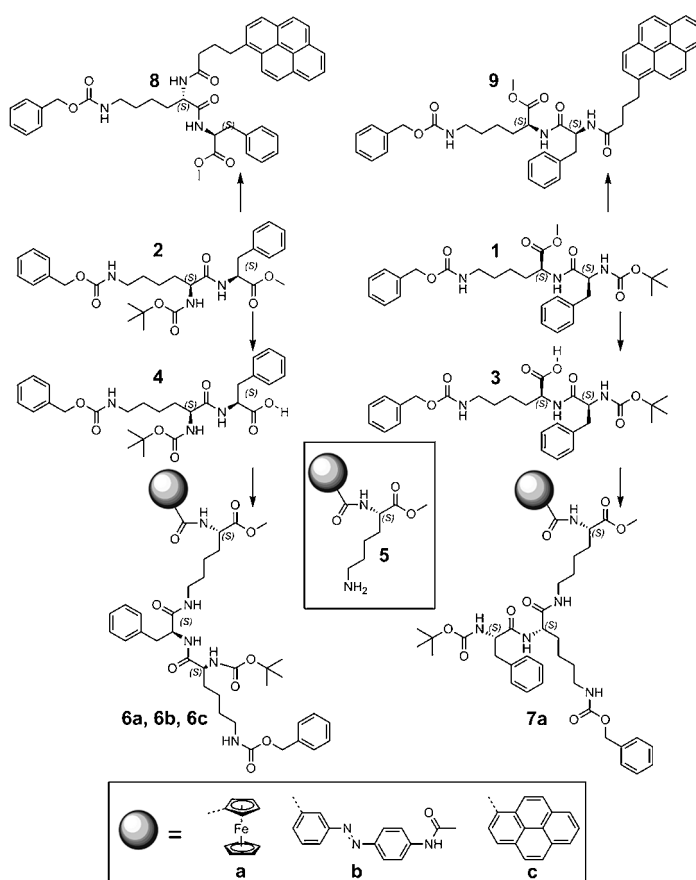
erved that the self-organization of the components can lead to highly ordered systems in which discrimination between compatible and non-compatible building blocks directs the effective organization of the chromophores and gives rise to the formation of an excited-state complex with exciplex-like emission. The current report may prove important in the development of organogel-based multicomponent smart devices.

Introduction

In the last two decades, low molecular weight gelators (LMWGs) have been extensively investigated owing to their advantages in the development of smart functional materials.^[1] Most often, one of the prerequisites for constructing new functional devices is the presence of multiple components in the same media.^[2] In nature, self-sorting is a common mechanism that allows the organization of multiple components to create functional macromolecules.^[3] The photosynthetic system is one of the most interesting examples of self-assembly in which peptides direct the arrangement of chromophores in a highly efficient manner.^[4] The remarkable properties of self-sorting biological architectures has been the driving force behind the ever increasing interest in artificial self-sorting systems.^[5] In this respect, amino acids and peptides can be useful building blocks for the development of biomimetic materials with programmed self-assembly.^[6] Self-healing gels that exhibit reversible redox, light- and sound-responsive switching can be attractive tools for the generation of new gel-based molecular devices. Despite extensive research in the field of supramolecular organogels, no strategy is yet known that solely relies on the self-assembly of ultra-short peptides to create various multi-stimuli-responsive organogels with self-healing and self-sorting properties. Moreover, transcription of such responsive properties from one molecule to another, using simple building blocks, is yet to be explored.

Herein, we report a facile method for the construction of various stimuli-responsive organogels that is driven by the

predictive self-assembly of ultra-short peptides. Moreover, the narcissistic self-sorting of the gelators has been exploited for the efficient co-assembly of a donor-acceptor dual-component gel as a simplified model for a supramolecular photo-conversion device.^[7] The effective organization of the chromophores was found to give rise to the formation of an excited-state complex with exciplex-like emission. Our strategy was based upon the evidence that Boc-L-Phe-L-Lys(Z)-OMe (Z = carboxybenzyl, **1**; Scheme 1) can undergo a folding transition in aromatic solvents, which leads to hierarchi-



Scheme 1. Synthetic scheme outlining the different stimuli-responsive organogelators reported here.

[a] R. Afrasiabi, Prof. Dr. H.-B. Kraatz
Department of Physical and Environmental Sciences
University of Toronto, 1265 Military Trail
Toronto, M1C 1A4 (Canada)
Fax: (+1) 416 287-7197
and
Department of Chemistry, University of Toronto
80 St George Street, Toronto, M5S 3H6 (Canada)
E-mail: bernie.kraatz@utoronto.ca

Supporting information for this article is available on the WWW under <http://dx.doi.org/10.1002/chem.201303116>.

cal self-assembly and gel formation.^[8] Consequently, we had envisioned that due to the inherent and predictable conformational changes of **1**, this molecule and its analogues can serve as synthons to provide a straightforward method for designing various stimuli-responsive smart organogels.

As an integral part of our strategy it was assumed that the successful incorporation of synthons **3** and **4** into the corresponding product conjugates (Scheme 1) will provide systems that exhibit a stimuli-responsiveness analogous to that observed in the parent dipeptides, namely, spontaneous self-assembly in aromatic solvents and a reversible responsive change to sonication and mechanical stress (self-healing). To examine the versatility of this strategy and extend the number of external signals that the resulting molecules were responsive to, the dipeptide synthons **3** and **4** were equipped with three different classes of responsive moieties: 1) ferrocene as an example for a redox-triggered response moiety;

2) azobenzene as an example for a light-responsive molecule, and 3) pyrene as a fluorescent moiety. The justification for using the mentioned molecules lays in their ability to function as molecular switches in a plethora of systems.^[9] Moreover, we were interested to study the intricate properties and behaviors associated with such systems, including self-sorting and supramolecular logic-gate operations.

The target molecules were synthesized following conventional solution-phase approaches for peptide synthesis and the structures were confirmed by using a range of spectroscopic approaches, including ¹H/¹³C NMR and IR spectroscopies and ESI-MS (see the Supporting Information). Three of the target molecules were obtained by coupling the C-terminus of Boc-L-Lys(Z)-L-Phe-OH (Z = carboxybenzyl, **4** in Scheme 1) to the ε-amino group of lysine-functionalized ferrocene, azobenzene, and pyrene derivatives (compound **5** in Scheme 1). To examine the effect of peptide sequence on

the properties of the gels, compound **7a** was also prepared by using synthon **3**, which has the reverse amino acid sequence compared with **4**.

Considering our previous knowledge of the helicogenic effect of aromatic solvents on peptide **1**, unless otherwise stated, toluene has been used as the solvent in all the below-mentioned studies. In tube-inversion experiments, the gelators displayed very strong gelation behavior and had no appreciable flow even at such low concentrations as 0.2–0.25 wt %, placing them in the class of super-gelators for toluene at ambient temperature. Importantly, sonication-triggered gelation, thermo-reversible gel-sol transition, and self-healing behavior was present in all conjugates of **1** and **2** (see the Supporting Information for conditions used for preparing the gels).

To ensure that the synthesized molecules did in fact inherit the folding behavior observed for the peptides **1** and **2**, compound **6a** was examined as a model to probe the transcription of programmed self-assembly. Figure 1 provides the results for NMR spectroscopic and UV/Vis data that support the self-organization of **6a** in toluene. In solvent titration ex-

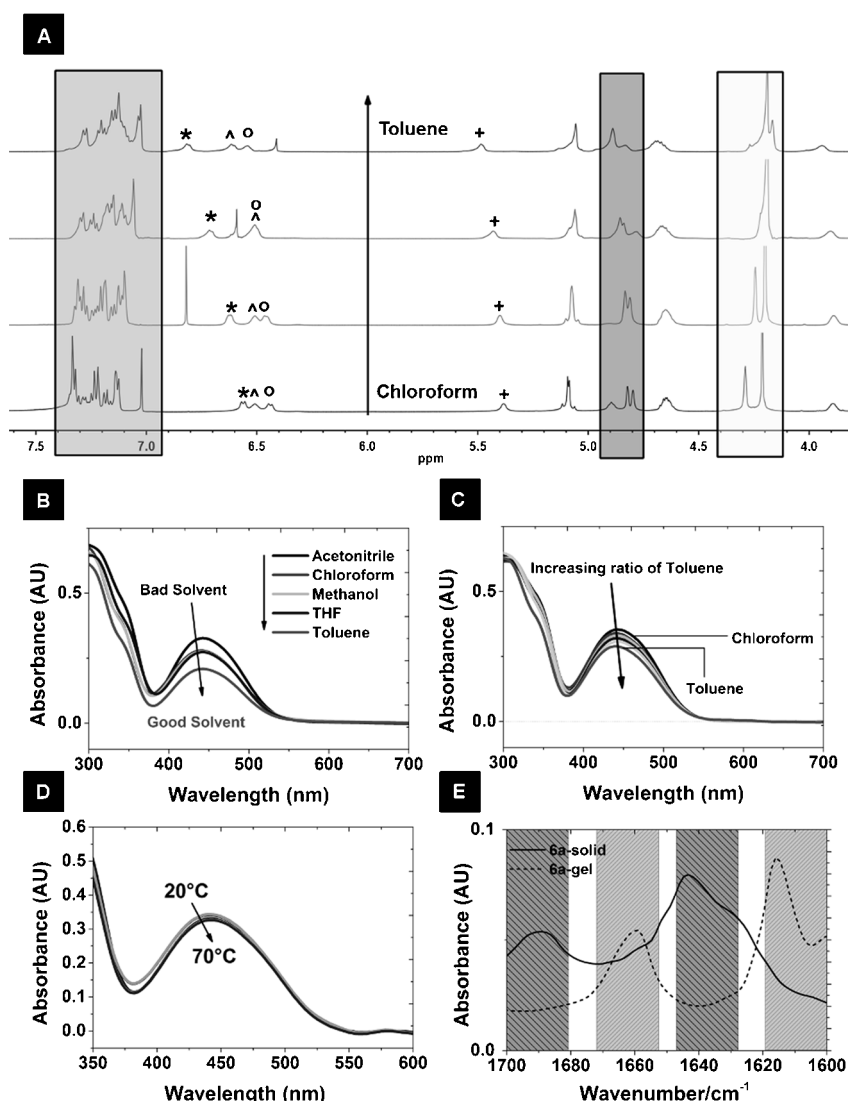


Figure 1. A) ¹H NMR spectra of **6a** in various ratios of chloroform/toluene (1:0, 2:1, 1:2, 0:1; total volume 0.6 mL). B) UV/Vis spectra of **6a** in different solvents. C) UV/Vis spectra of **6a** in various ratios of chloroform/toluene (1:0, 2:1, 1:2, 0:1). D) Thermal denaturation spectra for **6a**; E) FTIR Spectra of **6a**, solid state (solid line), gel state (dotted line).

periments, performed by recording the $^1\text{H NMR}$ spectroscopic signal as a function of solvent composition, compound **6a** demonstrated similar changes to those observed for **1**, including the downfield shift of amide proton resonances accompanied by the upfield shift of the proton signals in the aromatic region (Figure 1A). These variations in $^1\text{H NMR}$ spectra can be attributed to aggregation through π - π stacking. The solvent dependence of self-assembly in addition to the results from the solvent-denaturation experiments conducted by using UV/Vis spectroscopy (Figure 1B and C) were consistent with the folding of the structure in toluene, whereas hypochromic and hypsochromic effects relative to the chloroform solution were detected. On the other hand, temperature-dependent UV/Vis studies demonstrated reversible spectral changes between 20 to 70 °C, which complemented our previously mentioned results (Figure 1D). The FTIR spectra of the prepared compounds showed no bands at 3400 cm^{-1} for the solid or gel state, indicating that all the amide bonds were involved in intermolecular hydrogen-bonding. In the solid form, compound **6a** demonstrated a strong band at 1682 cm^{-1} . Interestingly, a shift in the amide I band centered around 1640 cm^{-1} was detected for **6a** in the gel state, which may indicate the formation of β -sheet conformation upon self-assembly (Figure 1E). In all the gel samples a band at around 1613 cm^{-1} was observed, which can be assigned to turn, helical, or irregular loop-like structures (see the Supporting Information for the complete FTIR spectra). Moreover, in temperature-dependent $^1\text{H NMR}$ experiments (Figure 2A for toluene gel of **6a**), a decrease in molecular motion was detected below 25 °C, which is evidenced by the absence of signals above $\delta = 3\text{ ppm}$. The peaks visible between $\delta = 0$ –3 ppm arise from alkyl groups, which are expected to have more mobility even at lower temperatures.

The ferrocene moiety is speculated to be buried inside the assembled structure due to the low intensity of related proton signals below 80 °C ($\leq T_{\text{gel}}$) (Figure 2A). The folding of the molecule to form a supramolecular polymer was also supported by circular dichroism (CD) spectroscopy, which shows the formation of a chiral supramolecular structure for the toluene gel of **6a** compared with the chloroform solution of the gelator in which the monomeric form is present (Figure 2B). The spontaneous self-assembly of **6a** in aromatic solvents was further supported by using temperature-dependent CD spectroscopy and scanning electron microscopy (SEM) experiments (see below), indicating the formation of stable and chiral assemblies in toluene. CD can be a potent technique for distinguishing the chiral arrangement of molecules in highly organized systems. The positive Cotton effects in the range 450–500 nm suggest a superhelical arrangement of respective chromophores in the gel state, induced by the molecular chirality of the synthon peptides (Figure 2C). To affirm the formation of supramolecular chirality, gels were subjected to thermal denaturation experiments. Upon increasing the temperature (20–80 °C), a decrease in the CD signal was detected that eventually diminished to zero at temperatures higher than 80 °C ($\geq T_{\text{gel}}$) (Fig-

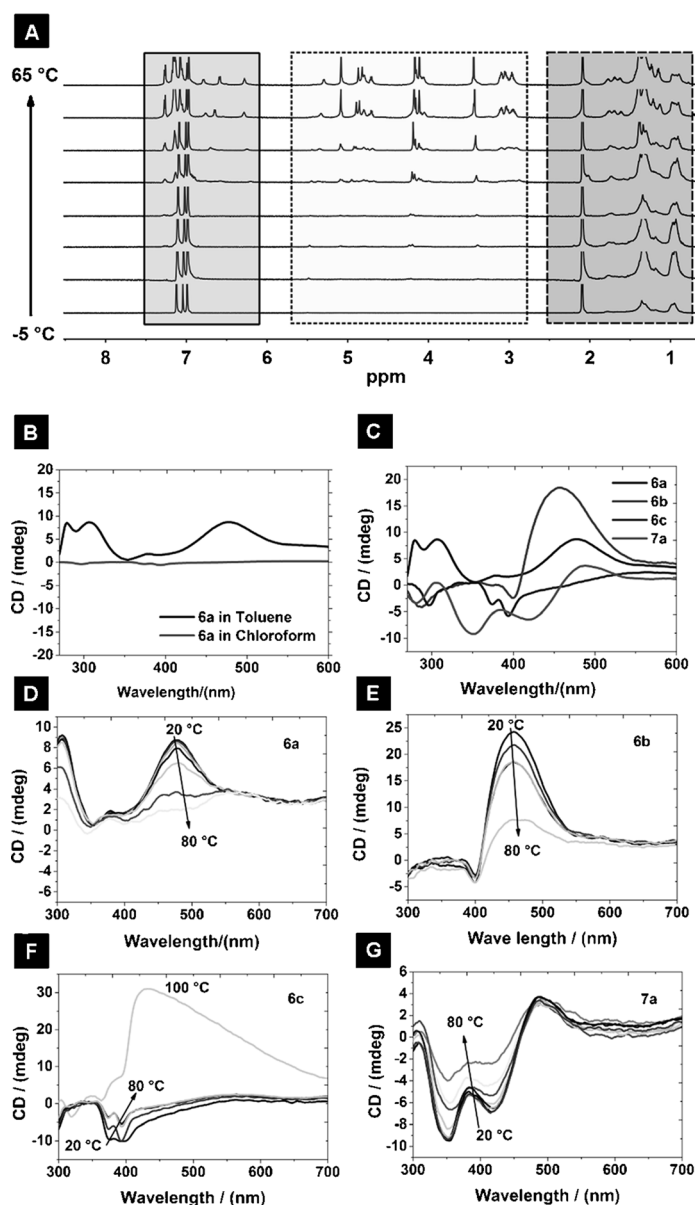


Figure 2. A) Temperature-dependent $^1\text{H NMR}$ spectra of **6a** gel in $[\text{D}_8]\text{toluene}$ (at the minimum gel concentration (mgc)). B) Circular dichroism spectra of **6a** in toluene and in chloroform. C) CD spectra of the prepared gels. D)–G) Temperature-dependent CD spectra of toluene gels of **6a**, **6b**, **6c**, and **7a** (a 0.5% gel sample has been investigated in all experiments).

ure 2D–G). Interestingly, in the case of organogelator **6c**, a chiroptical switching phenomenon was observed at 100 °C (Figure 2F).

It must be pointed out that the presence of self-healing ability is a key feature of the reported gels, which allows reconstitution of the damaged structure following the application of a destructive mechanical signal. To study the mechanical properties of the gels, rheological experiments were carried out (Figure 3A–C show representative data for **6a**, also see the Supporting Information for complete rheological experiments). The Winter–Chambon criterion for gela-

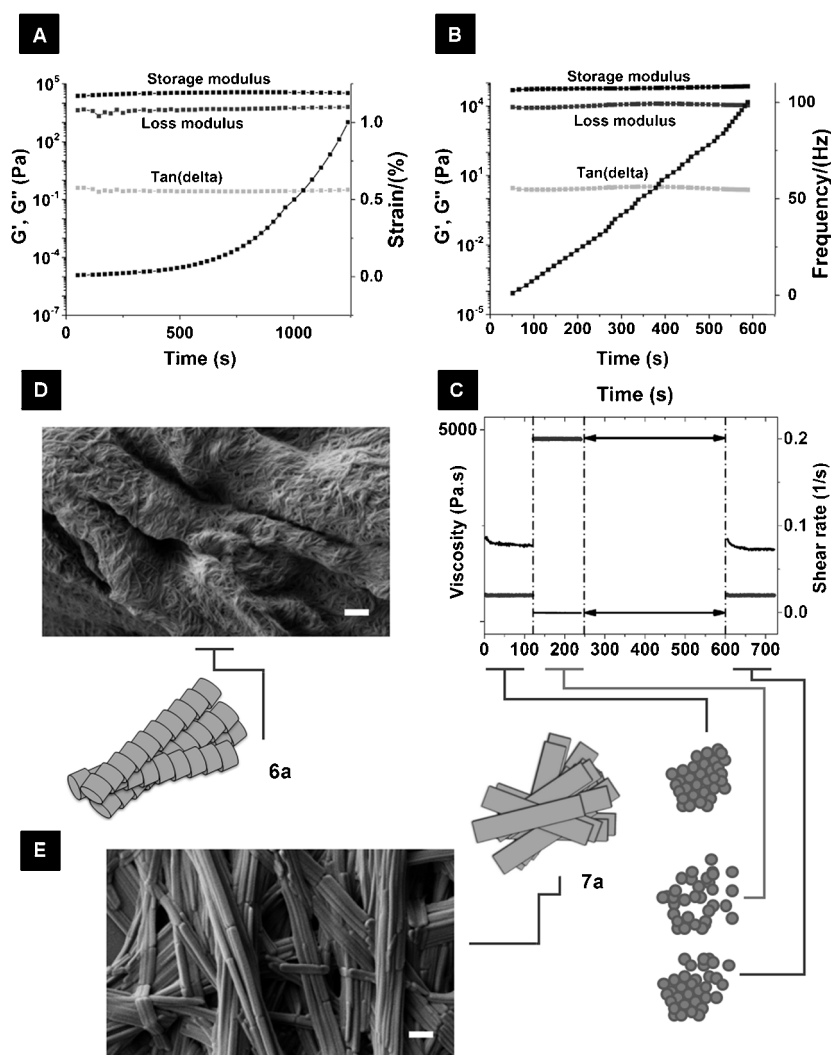


Figure 3. A) Strain-sweep experiment for **6a** at constant angular frequency of 1 Hz and strain ranging from 0–1%. B) Frequency-sweep experiment for **6a** at constant strain of 1% with angular frequency ranging from 1–100 rads^{-1} . C) Rheological experiment demonstrating changes in viscosity of toluene gel of **6a** in response to applied shear-rate stress. D) and E) FESEM micrographs of xerogels of **6a** and **7a** (scale bars indicate 100 nm).

tion points was used for determining the viscoelastic properties of the samples. Initially, strain-sweep experiments were carried out at angular frequency of 1 Hz and the changes in dynamic moduli were plotted with respect to an increasing strain amplitude (Figure 3A for **6a**). In all cases, the storage modulus (G') and loss modulus (G'') exhibited a very weak dependency on the strain amplitude and G' values exceed G'' by at least one order of magnitude, an indication of strong gel behavior. In frequency-sweep experiments, which were performed at constant strain of 1% and between 0.1 to 100 rads^{-1} (Figure 3B for **6a**), the gels showed a frequency-independent storage modulus. Next, the successful transfer of the self-healing property to the target molecules was evaluated (Figure 3C for **6a**). The gels were subjected to mechanical loading and the recovery of the network was monitored for each of the samples using different experiments.

Figure 3C demonstrates one cycle of breaking and recovery for the gel of **6a** based on changes in viscosity.

Field-emission electron microscopy (FESEM) images of the xerogels of **6a** and **7a** were investigated as models to elucidate the nanoscale morphology of the organogels (Figure 3D and E). Surprisingly, a difference in morphology was observed that may correlate directly to the difference in the sequence of amino acids in the parent synthons. Whereas nanofibers were found to constitute the network of **6a**, SEM images of **7a** showed the formation of nanorods/nanotapes. We believe this difference in nanostructure is yet another merit of our strategy that allows the transfer of information from the molecular level to the nanometer-level morphology.

As outlined before, the smart gels reported here were found to be responsive to thermal, mechanical, and sound signals. Moreover, as we had expected, this smart response to change was inherited from the parent synthons. However, to establish that our strategy could be extended to other systems it was necessary to investigate the responsive nature of the prepared gels to their specific signals. To be able to record the switching

behavior, spectroscopic changes were monitored for all the gels as a function of applied external signal. Firstly, the redox-responsive switching of the ferrocene gels was studied by using an oxidizing agent ($[\text{Fe}(\text{ClO}_4)_3]$) to oxidize the ferrocene group (Fc) to ferrocenium (Fc^+). A few drops of the $[\text{Fe}(\text{ClO}_4)_3]$ solution in acetone was added on top of the gel, which induced concurrent oxidation of the ferrocene unit accompanied by a gel-to-solution transition after 3–5 h. Our results demonstrate that due to the partial solubility of the oxidized form of the gelator in toluene, the current system suffers from the gradual precipitation of the gelator after oxidation and hence limits the time the oxidized solution is stable. Work is currently underway to eliminate this problem by designing ferrocene-peptide conjugates capable of forming gels in more polar solvent. Consequently, redox sol-gel transitions were carried out on the gel of **6a** or **7a** in a mixture of acetone and toluene. Oxidation of the gel leads to

a change in the color of the sample from light-orange to dark-blue (characteristic for Fc^+ ; Figure 4A and 4E, left). The solution-to-gel transition was made possible through the introduction of a reducing agent (ascorbic acid) followed by heating/sonication to reduce Fc^+ to Fc (Figure 4A and 4E, left). Despite the feasibility of carrying out chemical-redox reactions, a decrease in gel strength was observed after two cycles for both **6a** and **7a** (the chemically reconsti-

tuted gel is unstable and collapses after 2 min). Next, we turned our attention to the azobenzene derivative of **4**. The viscous loose gel of **6b** was irradiated with UV light (365 nm) and the gradual changes in UV/Vis spectra were recorded (Figure 4B). A 0.5% gel sample of **6b** was found to lose its mechanical properties and collapse after the application of UV light for 30 min. Gel regeneration and recovery was possible by exposing the solution to visible light for 60 min or sonication for 10 min (see Figure 4B and E). Finally, fluorescence switching was examined for **6c** under thermal conditions and between sol and gel states. As mentioned before, variable-temperature CD experiments indicated a change in chiroptical properties when **6c** transitioned from the gel-to-sol state. Consequently, in the case of **6c**, an enhancement in fluorescence was observed upon gel formation that is thought to arise from aggregation-induced enhanced emission phenomenon (AIEE) (Figure 4C and D). The above results demonstrate the generality of our strategy as a straightforward method for constructing various stimuli-responsive organogels.

Upon successful incorporation of the synthons and tailoring of the desired properties into the target molecules, their ability to logically and uniformly co-assemble in a hybrid system was examined. As a simple model for a supramolecular photo-conversion device, mixtures of the ferrocene and pyrene gelators were selected for studying electron/energy transfer in the dual-component organogels. The extent of quenching of the excited state of pyrene by ferrocene was deemed to provide a measure of the distance between the supramolecular dyad and the effectiveness of the co-assembly. In addition, it was assumed that the self-sorting behavior of the gels can provide a method for understanding the relative spatial orientation of the donor and acceptor chromophores.

The possibility of a self-sorting mechanism was based on the observation that various mixtures of **1** and **2** with different ratios were incapable of gel formation in toluene and the presence of both species in the same mixture, even at very low concentrations, hindered organization under thermal conditions. Interestingly, the same mixtures were also incapable of gel formation in response to sonication unless one of the components was available in very high concentrations. Despite the attractive features of **6c** for potential applications in constructing gels with logic-gate properties, the thermal fluorescence switching of this derivative was thought to complicate the understanding of the interactions in the dual-component gels. To simplify the systems, we synthesized two new gelators by conjugating a pyrene derivative to the N-terminus of **1** and **2** (compounds **8** and **9**, respectively, in Scheme 1). The new gelators exhibited very little change in fluorescence intensity or position of the peaks between the solution and the gel state (see the Supporting Information). These fluorescence derivatives were then used to investigate the co-assembly of the ferrocene and pyrene gels under thermal (heating-cooling) and sonication (heating-sonication) conditions. Experiments were carried out by mixing the components under conditions in

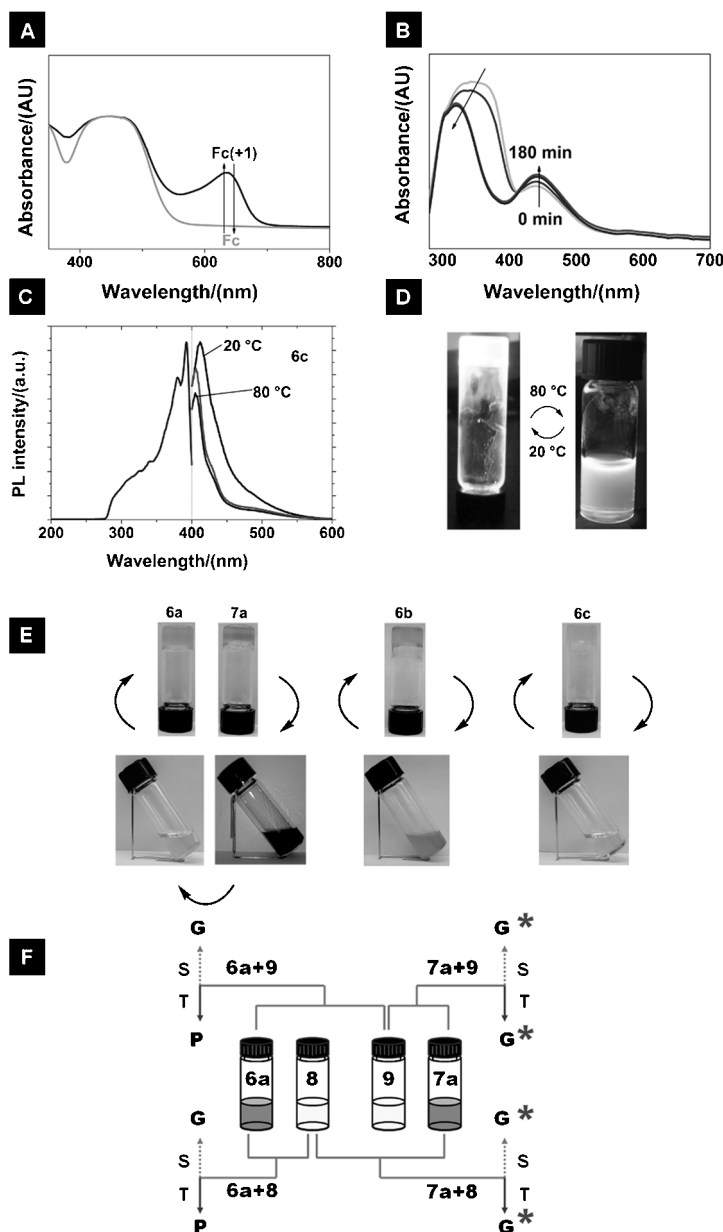


Figure 4. A) Reversible oxidation and reduction of the **6a/7a** performed in a mixture of acetone/toluene. B) photo-induced switching of **6b**. C) Absorption and emission spectra for **6c** demonstrating changes in emission at different temperatures. D) Photographs of **6c** in gel and solution state. E) Photographs of phase transitions in the prepared gels in response to: redox (left), light (middle), heat (right); F) Schematic summarization of the results for the mixtures under different conditions: sonication (S), thermal (T), gelation (G), precipitation (P), exciplex-like emission (*).

which the wt% of each component was less than half of their individual minimum gel concentration (mgc) values to maximize the consequences of constructive or destructive interactions between the two components. Figure 4F summarizes the results for the co-gels formed under thermal- and sonication-induced conditions. Surprisingly, the two-component organogels of ferrocene and pyrene (**6a+8**, **6a+9** and **7a+8**, **7a+9**) exhibited a similar behavior as that of mixtures of **1** and **2** under thermal conditions. A narcissistic self-sorting response was observed, which was driven by the amino acid sequence of the synthons. Mixtures of the ferrocene and pyrene gelators only exhibited co-gelation after heating and cooling when the two components had the same amino acid sequence (**6a+8** and **7a+9**). On the other hand, selective and gradual aggregation/precipitation of the components was noticed when co-assembly was not favored. Interestingly, despite a delay in gelation time for **7a+8** and **6a+9**, application of sonication resulted in gel formation in these mixtures although they did not possess the same sequence of amino acids.

SEM images revealed a fibrous morphology for xerogels of **8** and **9**, which lack any vivid chiral features (Figure 5A and B). Characterization of **6a+8** and **7a+9** showed subtle changes in the morphology of the samples compared with **6a** and **7a**, which can be attributed to the self-recognition of **8** and **9** by their respective co-gelators. To investigate the presence of a self-sorting phenomena, the nanoscale morphology of **7a+8** was also investigated. This mixture of gelators was selected due to the difference in morphology between **7a** (nanotape) and **9** (nanofiber) compared with **6a+9**, in which both of the gelators have nanofiber morphology. SEM images of the mixture of **7a** and **8** with a molar ratio of 0.25 and 1 for the gelators (Figure 5E) showed the formation of a heterogeneous network that was dominated by thin nanofibers of **8**. In this heterogeneous network, the nanotapes that were formed by **7a** were also observed but had a lower abundance. The predominance of nanofiber morphology in comparison to nanotape structure is thought to arise from the higher molar ratio of **8** compared with **7a**. Considering the fact that SEM investigations failed to prove any change in the morphological features (in comparison to the individual gelators) for the thermally formed **6a+8** and sonication induced **6a+9** (Figure 5F), CD experiments were carried out to evaluate the possibility of self-recognition in these mixtures. The CD spectra of the mentioned mixtures were investigated in samples with varying molar ratios of **6a** relative to a fixed amount of **8** or **9** (Figure 5G). Bisignate Cotton effects were observed in the CD spectra of both **6a+8** and **6a+9** but the amplitude value was greater for **6a+8** and this mixture exhibited a signal that could be indicative of exciton coupling between two chromophores (two pyrenes or pyrene and ferrocene).^[10]

Interestingly, the CD spectra for 2:1 molar ratio mixtures of **6a** with **8** or **9** were found to be significantly different in the 300–400 nm region (Figure 5G). At this molar ratio, the CD spectrum for **6a+9** is mainly composed of the signals from **6a** in the 400–600 nm region and the peaks in 300–

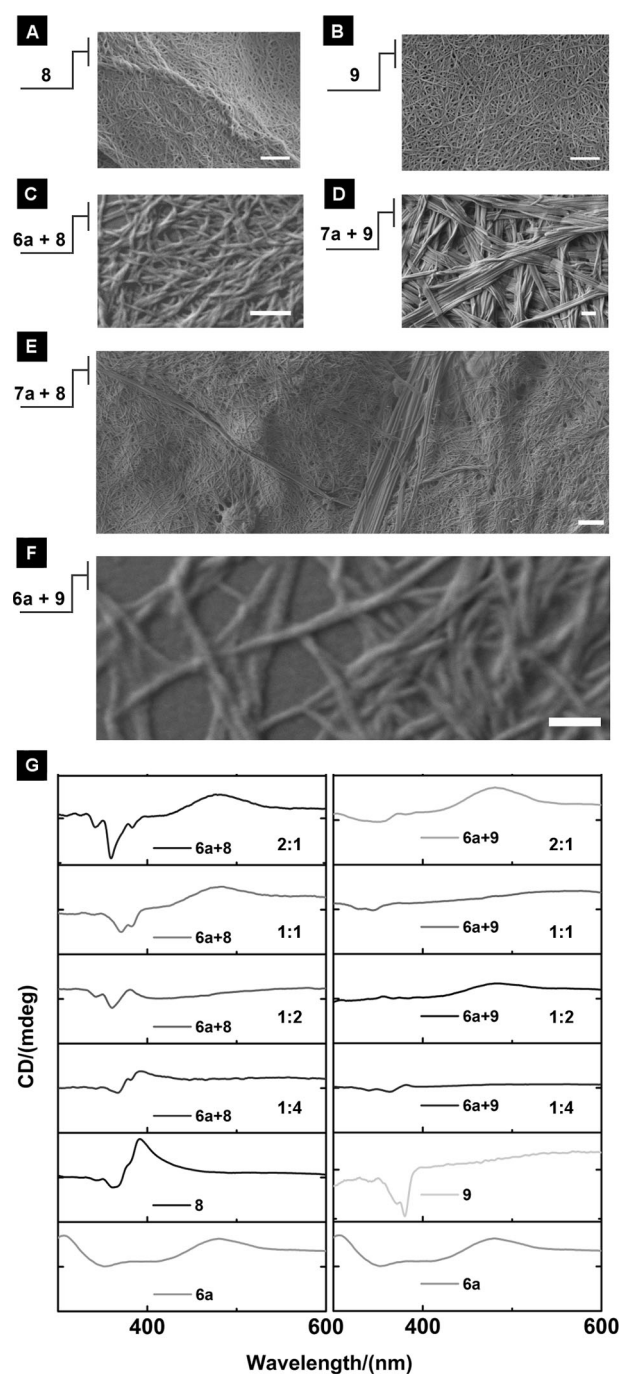


Figure 5. A)–F) FESEM micrographs of xerogels of: A) **8** (scale bar indicates 1 μ m); B) **9** (scale bar indicates 1 μ m); C) **6a+8** (scale bar indicates 100 nm); D) **7a+9** (scale bar indicates 100 nm); E) **7a+8** (scale bar indicates 1 μ m); F) **6a+9** (scale bar indicates 100 nm). G) CD spectra of mixtures of **6a** with **8** and **9** with increasing molar ratio of **6a** and constant amount of **8** and **9** (all spectra are reported in the -10 – $+10$ mdeg range).

400 nm were highly attenuated. This observation could indicate that in the presence of **6a**, the ability of **9** to undergo self-assembly is highly suppressed and this component is excluded from the network of **6a**. On the other hand, the same results could be interpreted by the formation of two

types of fibers by **6a** and **9**, which have the opposite helical handedness, resulting in a very weak CD signal upon application of sonication, which allows the fibers to intertwine. Both interpretations are in accordance with the predominance of the CD spectra by the signals from the component with the higher molar ratio. On the contrary, a 2:1 mixture of **6a** and **8** appeared to have the signals related to the ferrocene and pyrene chromophores (Figure 5G). More importantly, the signals observed in the 300–400 nm region for **6a+8** mixture showed an opposite CD signal compared with the signals from **8** alone. Considering the enhancement of signals for the pyrene component compared with the mixture **6a+9**, we speculate that the observed changes for the CD spectra of **6a+8** are the direct consequence of self-recognition between **6a** and **8**. Based on the above-mentioned results, three mechanisms can be proposed for how the interactions between **6a** and **8** or **9** take place (Figure 6A–C). To further investigate the interactions responsible for gel formation in case of **6a+8**, variable-temperature ^1H NMR experiments were performed on the toluene gel of this mixture. It was assumed that ^1H NMR experiments can provide information regarding the interaction between the components and clarify if **6a** and **8** self-assemble independently into fibers of a single component (Figure 6C) or form a single fiber that consists of both of the components (Figure 6A and B). Comparison of the temperature-dependent changes in the spectra of **6a** and **6a+8** demonstrate slight changes in the position of the amide-proton peaks and an increase in hydrogen bonding, supported by the downfield shift of amide-proton signals. Additionally, it was found that the signals due to the ferrocene unit in the $\delta=4.5\text{--}5$ ppm region exhibit an increase in the splitting between the two peaks associated with the substituted-cyclopentadienyl ring of ferrocene (Figure 6D). Since the observed changes for **6a+8** can be related to the presence of **6a** and **8** molecules in close proximity, we speculate that in a mixture of **6a+8** the organization mainly follows the schematic representation in Figure 6A or B, with a lower possibility through the path shown in Figure 6B. However, the organization of the components in **6a+9** is speculated to follow a similar process as depicted in Figure 6C. To gain insight into the underlying interactions between the chromophoric moieties, vibrational circular dichroism (VCD) experiments were performed. VCD results demonstrate differences in the signals observed for **6a+8** and **7a+9** (Figure 7A). Comparison between the VCD signals for the mixed gels that had formed under thermal conditions, and had the same peptide sequence, with the sonication-induced gels, which lacked resemblance in the peptide sequence, demonstrated clear differences in the intensity of the peaks in the region $1650\text{--}1680\text{ cm}^{-1}$ (Figure 7A). The amplification of the VCD signals in this region for **6a+8** and **7a+9** is thought to arise from the organization of the molecules in a highly ordered manner, which results in the formation of well-ordered architectures. The peaks observed in the $1650\text{--}1680\text{ cm}^{-1}$ region can be attributed to the formation of β -structures in the case of **6a+8** and **7a+9**, whereas the differences in the

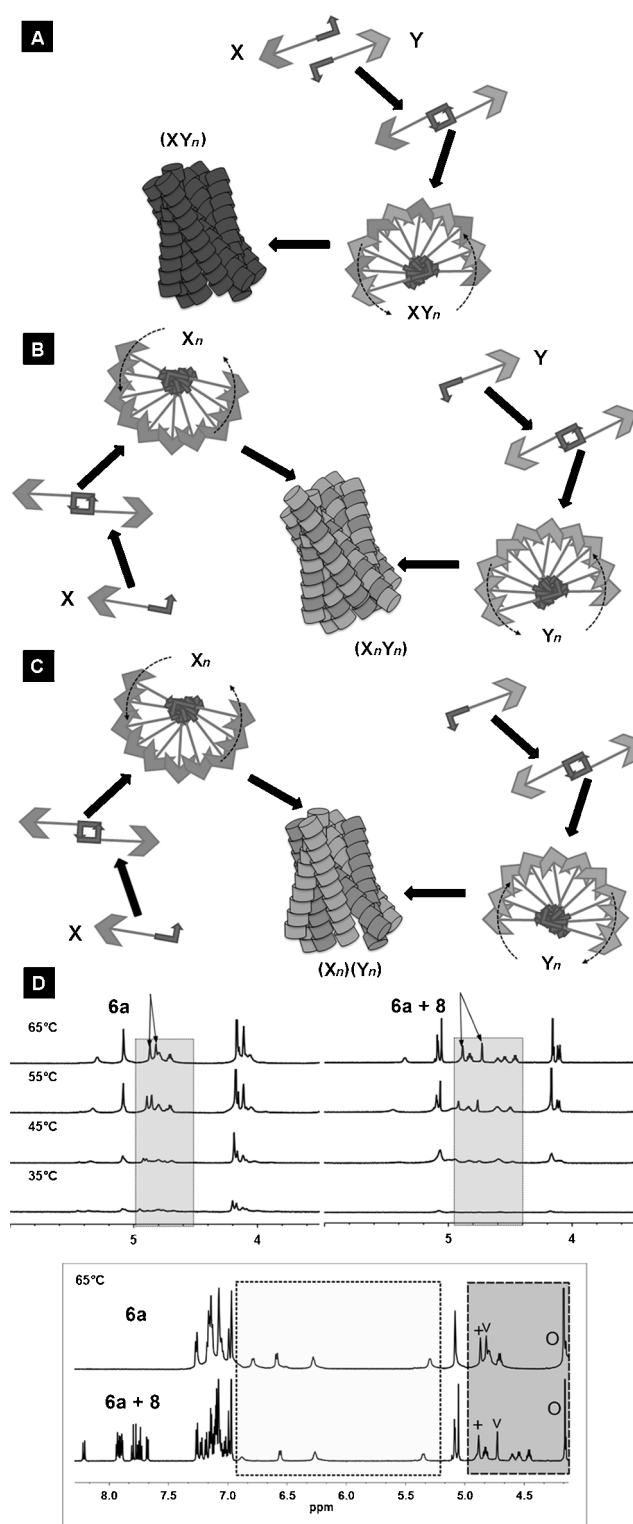


Figure 6. A)–C) Speculated cartoon representation of organization of molecules in a mixture of **6a** with **8** or **9** (see the Supporting Information for the color version of this figure). D) Temperature-dependent ^1H NMR spectra of **6a** and **6a+8** that show differences in the position of the peaks attributed to substituted-cyclopentadienyl ring of ferrocene (represented by + and V, whereas O is related to the unsubstituted-cyclopentadienyl ring).

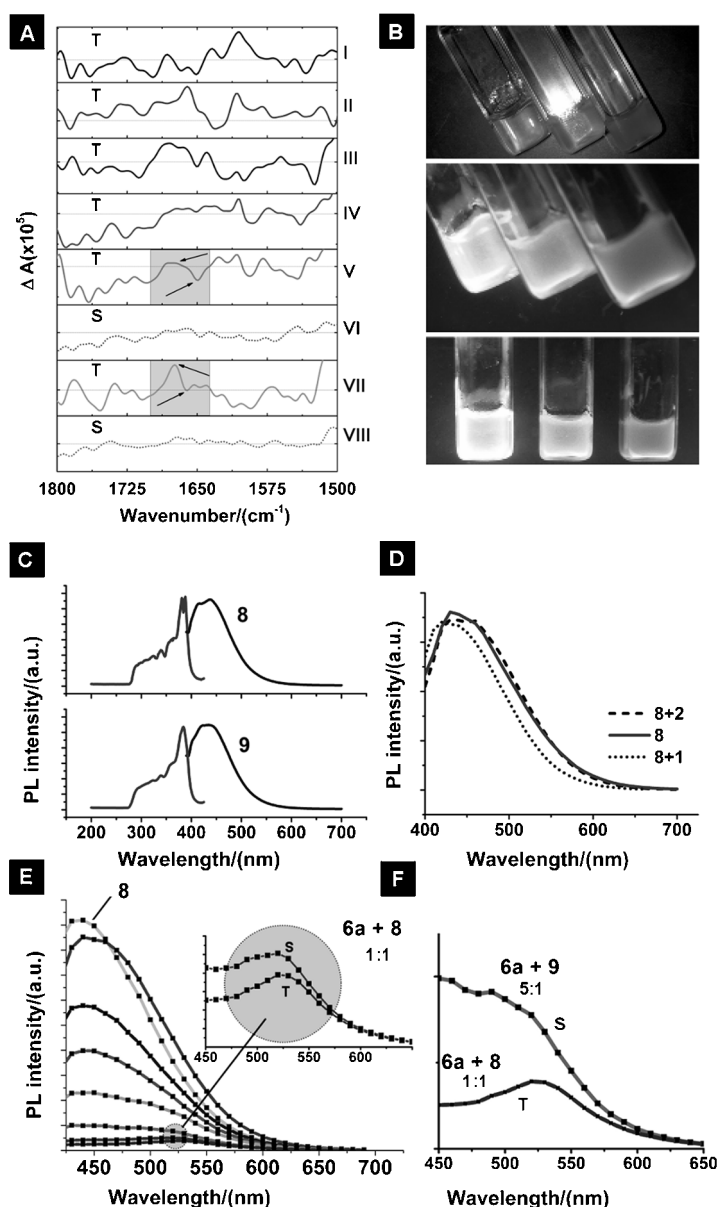


Figure 7. A) Vibrational circular dichroism spectra for the gels and mixed gels prepared under thermal (T) and sonication (S) conditions: (I) **6a**, (II) **7a**, (III) **9**, (IV) **8**, (V) **7a+9** (1:1), (VI) **7a+8** (1:1), (VII) **6a+8** (1:1), (VIII) **6a+9** (1:1). B) Photographs of the **6a+8** co-gel showing the quenching of fluorescence as the ratio of the quencher (**6a**) is increased (ratio of the quencher from left to right: 0:1, 0.5:1, 1:1). C) Absorption and emission spectra for **8** and **9** (excitation at 400 nm). D) Emission spectra for **8**, **8+1** (S) and **8+2** (S) (excitation at 400 nm). E) Fluorescence spectra of **6a+8** mixture as a function of increasing ratio of **6a** (0:1 to 1:1). Inset shows the difference in fluorescence between thermally and sonication induced 1:1 molar ratio co-gels of **6a+8**. (excitation at 400 nm). F) Fluorescence spectra for a 5:1 co-gel of **6a+9** formed after sonication for 15 min.

sign and position of the peaks is compatible with a distinction in the modes of interaction and the supramolecular organization of the components.^[11]

Next, fluorescence experiments were carried out to investigate the efficiency of the quenching for the mixed gels.

The quenching was found to be most effective for the co-gels prepared under thermal conditions and when the gels contained the same peptide synthons (**6a+8** and **7a+9**). Figure 7B demonstrates the decrease in fluorescence for **8** as the ratio of **6a** is increased. To investigate the source of quenching and confirm that the electron/energy transfer between the chromophores is responsible for the decrease in fluorescence, toluene gels of **8** and **9** were investigated in absence of **6a** and **7a** (Figure 7C). Next, we investigated the possibility of quenching in mixtures of **8** with **1** and **2**. Figure 7D demonstrates the minor changes observed in the fluorescence of **8** in co-gels of this gelator with **1** and **2**. These results indicate that the source of quenching is due to interaction between the ferrocene and pyrene chromophores and is not the result of self-quenching or quenching by the peptide segment alone.

Interestingly, co-gels of the pyrene and ferrocene gelators with the same parent dipeptide showed exciplex-like emission in equimolar mixtures under thermal and sonication-induced conditions (Figure 7E for **6a+8**). Very little difference was observed in the quenching of fluorescence for **6a+8** and **7a+9** prepared under sonication or thermal conditions (see the inset of Figure 7C for **6a+8**). However, for the co-gels **6a+9** and **7a+8** prepared under sonication, an exciplex-like emission was first detected in 5:1 molar ratio mixtures of the two components (Figure 7F).

We attribute the difference observed for the effectiveness of quenching in the co-gels formed under thermal and sonication-induced conditions to originate from the dissimilarity of the organization of molecules in the two systems. Under thermal conditions, unfavorable interactions avoid gel formation for **6a+9** and **7a+8**, and a narcissistic self-sorting behavior is observed, which is due to the lack of interaction between the fibers that impedes gel formation and results in precipitation of one or both of the components. On the other hand, when the same mixtures are sonicated (**6a+9** and **7a+8**), the fibers formed by each component is forced to interact with the fibers from the second component and this allows gel formation. The inefficiency of the quenching for **6a+9** and **7a+8** under sonication and the requirement for higher ratios of the quencher can then be related to the difference between fiber–fiber quenching (Figure 6C) compared with molecule–molecule quenching speculated for **6a+8** and **7a+9** co-gels (Figure 6A).

Conclusion

We have demonstrated here a facile bottom-up strategy for the synthesis of various stimuli-responsive smart organogelators based on the predictive self-assembly of analogous dipeptides. Our results show that the successful incorporation of the synthon peptides permits the transcription of information and responsive behavior to the target molecules. The prepared gels not only exhibit self-healing and a reversible sol-to-gel transition towards sonication, but also have self-sorting properties. As a proof of concept, these characteris-

tics were exploited in a simplified model for a light-harvesting system. In donor–acceptor co-gels formed under thermal conditions, narcissistic self-sorting resulted in effective quenching and was accompanied by an exciplex-like emission from the mixed gels. The results presented here highlight the extremely useful nature of ultra-short peptides in developing smart functional materials. The reported strategy may prove important in the development of responsive organogels and multicomponent smart devices.

Acknowledgements

Financial support from NSERC and the University of Toronto is gratefully acknowledged. We thank Tony Adamo for help with data collection and acknowledge the Nanofabrication facility at Western University Canada for FESEM imaging.

- [1] a) B.-K. An, D.-S. Lee, J.-S. Lee, Y.-S. Park, H.-S. Song, S. Y. Park, *J. Am. Chem. Soc.* **2004**, *126*, 10232–10233; b) K. M. Anderson, G. M. Day, M. J. Paterson, P. Byrne, N. Clarke, J. W. Steed, *Angew. Chem.* **2008**, *120*, 1074–1078; c) D. Bardelang, F. Camerel, J. C. Margeson, D. M. Leek, M. Schmutz, M. B. Zaman, K. Yu, D. V. Soldatov, R. Ziessel, C. I. Ratcliffe, J. A. Ripmeester, *J. Am. Chem. Soc.* **2008**, *130*, 3313–3315; d) Y. Gao, Y. Kuang, Z.-F. Guo, Z. Guo, I. J. Krauss, B. Xu, *J. Am. Chem. Soc.* **2009**, *131*, 13576–13577; e) A. Gopal, M. Hifsudheen, S. Furumi, M. Takeuchi, A. Ajayaghosh, *Angew. Chem.* **2012**, *124*, 10657–10661; *Angew. Chem. Int. Ed.* **2012**, *51*, 10505–10509; f) A. R. Hirst, B. Escuder, J. F. Miravet, D. K. Smith, *Angew. Chem.* **2008**, *120*, 8122–8139; *Angew. Chem. Int. Ed.* **2008**, *47*, 8002–8018; g) A. R. Hirst, S. Roy, M. Arora, A. K. Das, N. Hodson, P. Murray, S. Marshall, N. Javid, J. Sefcik, J. Boekhoven, J. H. van Esch, S. Santabarbara, N. T. Hunt, R. V. Ulijn, *Nat. Chem.* **2010**, *2*, 1089–1094; h) S. R. Jadhav, P. K. Vemula, R. Kumar, S. R. Raghavan, G. John, *Angew. Chem.* **2010**, *122*, 7861–7864; *Angew. Chem. Int. Ed.* **2010**, *49*, 7695–7698; i) K. T. Kim, C. Park, G. W. M. Vandermeulen, D. A. Rider, C. Kim, M. A. Winnik, I. Manners, *Angew. Chem.* **2005**, *117*, 8178–8182; *Angew. Chem. Int. Ed.* **2005**, *44*, 7964–7968; j) R. Klajn, P. J. Wesson, K. J. M. Bishop, B. A. Grzybowski, *Angew. Chem.* **2009**, *121*, 7169–7173; *Angew. Chem. Int. Ed.* **2009**, *48*, 7035–7039; k) J. Liu, P. He, J. Yan, X. Fang, J. Peng, K. Liu, Y. Fang, *Adv. Mater.* **2008**, *20*, 2508–2511; l) P. Mukhopadhyay, Y. Iwashita, M. Shirakawa, S.-i. Kawano, N. Fujita, S. Shinkai, *Angew. Chem.* **2006**, *118*, 1622–1625; *Angew. Chem. Int. Ed.* **2006**, *45*, 1592–1595; m) J. Puigmartí-Luis, V. Laukhin, Á. Pérez del Pino, J. Vidal-Gancedo, C. Rovira, E. Laukhina, D. B. Amabilino, *Angew. Chem.* **2007**, *119*, 242–245; *Angew. Chem. Int. Ed.* **2007**, *46*, 238–241; n) K. V. Rao, K. K. R. Datta, M. Eswaramoorthy, S. J. George, *Angew. Chem.* **2011**, *123*, 1211–1216; *Angew. Chem. Int. Ed.* **2011**, *50*, 1179–1184; o) K. Sugiyasu, N. Fujita, S. Shinkai, *Angew. Chem.* **2004**, *116*, 1249–1253; *Angew. Chem. Int. Ed.* **2004**, *43*, 1229–1233; p) J. Wu, T. Yi, T. Shu, M. Yu, Z. Zhou, M. Xu, Y. Zhou, H. Zhang, J. Han, F. Li, C. Huang, *Angew. Chem.* **2008**, *120*, 1079–1083; *Angew. Chem. Int. Ed.* **2008**, *47*, 1063–1067; q) S. Yagai, M. Ishii, T. Karatsu, A. Kitamura, *Angew. Chem.* **2007**, *119*, 8151–8155; *Angew. Chem. Int. Ed.* **2007**, *46*, 8005–8009; r) Y. Zhang, B. Zhang, Y. Kuang, Y. Gao, J. Shi, X. X. Zhang, B. Xu, *J. Am. Chem. Soc.* **2013**, *135*, 5008–5011.
- [2] a) Y. Ren, W. H. Kan, V. Thangadurai, T. Baumgartner, *Angew. Chem.* **2012**, *124*, 4031–4035; *Angew. Chem. Int. Ed.* **2012**, *51*, 3964–3968; b) M. Nakahata, Y. Takashima, H. Yamaguchi, A. Harada, *Nat. Commun.* **2011**, *2*, 511; c) J. W. Chung, S.-J. Yoon, S.-J. Lim, B.-K. An, S. Y. Park, *Angew. Chem.* **2009**, *121*, 7164–7168; *Angew. Chem. Int. Ed.* **2009**, *48*, 7030–7034; d) T. Daeneke, T.-H. Kwon, A. B. Holmes, N. W. Duffy, U. Bach, L. Spiccia, *Nat. Chem.* **2011**, *3*, 211–215; e) W. Edwards, D. K. Smith, *J. Am. Chem. Soc.* **2013**; f) F. G. Brunetti, C. Romero-Nieto, J. López-Andarias, C. Atienza, J. L. López, D. M. Guldí, N. Martín, *Angew. Chem.* **2013**, *125*, 2236–2240; *Angew. Chem. Int. Ed.* **2013**, *52*, 2180–2184; g) R. Amemiya, M. Mizutani, M. Yamaguchi, *Angew. Chem.* **2010**, *122*, 2039–2043; *Angew. Chem. Int. Ed.* **2010**, *49*, 1995–1999.
- [3] a) A. Wu, L. Isaacs, *J. Am. Chem. Soc.* **2003**, *125*, 4831–4835; b) P. Mukhopadhyay, A. Wu, L. Isaacs, *J. Org. Chem.* **2004**, *69*, 6157–6164; c) J. R. Moffat, D. K. Smith, *Chem. Commun.* **2009**, *0*, 316–318; d) M. M. Safont-Sempere, G. Fernández, F. Würthner, *Chem. Rev.* **2011**, *111*, 5784–5814; e) Y. Rudzevich, V. Rudzevich, F. Klautzsch, C. A. Schalley, V. Böhmer, *Angew. Chem.* **2009**, *121*, 3925–3929; *Angew. Chem. Int. Ed.* **2009**, *48*, 3867–3871; f) A. Wicklein, S. Ghosh, M. Sommer, F. Würthner, M. Thelakkat, *ACS Nano* **2009**, *3*, 1107–1114.
- [4] a) J. H. Kim, M. Lee, J. S. Lee, C. B. Park, *Angew. Chem.* **2012**, *124*, 532–535; *Angew. Chem. Int. Ed.* **2012**, *51*, 517–520; b) P. D. Frischmann, K. Mahata, F. Würthner, *Chem. Soc. Rev.* **2013**, *42*, 1847–1870.
- [5] a) A. Pal, S. Karthikeyan, R. P. Sijbesma, *J. Am. Chem. Soc.* **2010**, *132*, 7842–7843; b) L. E. Buerkle, S. J. Rowan, *Chem. Soc. Rev.* **2012**, *41*, 6089–6102.
- [6] a) M. Sarikaya, C. Tamerler, A. K. Y. Jen, K. Schulten, F. Baneyx, *Nat. Mater.* **2003**, *2*, 577–585; b) T. Aida, E. W. Meijer, S. I. Stupp, *Science* **2012**, *335*, 813–817; c) G. Angelici, G. Falini, H.-J. Hofmann, D. Huster, M. Monari, C. Tomasini, *Angew. Chem.* **2008**, *120*, 8195–8198; *Angew. Chem. Int. Ed.* **2008**, *47*, 8075–8078; d) D. M. Ryan, T. M. Doran, B. L. Nilsson, *Chem. Commun.* **2011**, *47*, 475–477; e) K. L. Morris, L. Chen, J. Raeburn, O. R. Sellick, P. Cotanda, A. Paul, P. C. Griffiths, S. M. King, R. K. O'Reilly, L. C. Serpell, D. J. Adams, *Nat Commun* **2013**, *4*, 1480; f) Y. Liu, Y. Yang, C. Wang, X. Zhao, *Nanoscale* **2013**, *5*, 6413–6421.
- [7] S. S. Babu, S. Prasanthkumar, A. Ajayaghosh, *Angew. Chem.* **2012**, *124*, 1800–1810; *Angew. Chem. Int. Ed.* **2012**, *51*, 1766–1776.
- [8] R. Afrasiabi, H.-B. Kraatz, *Chem. Eur. J.* **2013**, *19*, 1769–1777.
- [9] a) S. Samanta, C. Qin, A. J. Lough, G. A. Woolley, *Angew. Chem.* **2012**, *124*, 6558–6561; *Angew. Chem. Int. Ed.* **2012**, *51*, 6452–6455; b) M. Tropiano, N. L. Kilah, M. Morten, H. Rahman, J. J. Davis, P. D. Beer, S. Faulkner, *J. Am. Chem. Soc.* **2011**, *133*, 11847–11849; c) R. Zhang, Z. Wang, Y. Wu, H. Fu, J. Yao, *Org. Lett.* **2008**, *10*, 3065–3068; d) S.-n. Uno, C. Dohno, H. Bittermann, V. L. Malinovsky, R. Häner, K. Nakatani, *Angew. Chem.* **2009**, *121*, 7498–7501; e) D. Margulies, C. E. Felder, G. Melman, A. Shanzer, *J. Am. Chem. Soc.* **2007**, *129*, 347–354; f) S. Amemori, K. Kokado, K. Sada, *Angew. Chem.* **2013**, *125*, 4268–4272; *Angew. Chem. Int. Ed.* **2013**, *52*, 4174–4178; g) G. Haberhauer, C. Kallweit, C. Wölper, D. Bläser, *Angew. Chem.* **2013**, *125*, 8033–8036; *Angew. Chem. Int. Ed.* **2013**, *52*, 7879–7882; h) M. Nakahata, Y. Takashima, A. Hashidzume, A. Harada, *Angew. Chem.* **2013**, *125*, 5843–5847; *Angew. Chem. Int. Ed.* **2013**, *52*, 5731–5735; i) P. Fatás, J. Bachl, S. Oehm, A. I. Jiménez, C. Cativiela, D. Díaz Díaz, *Chem. Eur. J.* **2013**, *19*, 8861–8874; j) C.-S. Chen, X.-D. Xu, S.-Y. Li, R.-X. Zhuo, X.-Z. Zhang, *Nanoscale* **2013**, *5*, 6270–6274.
- [10] a) N. Berova, L. D. Bari, G. Pescitelli, *Chem. Soc. Rev.* **2007**, *36*, 914–931; b) P. Ivicoli, H. Xu, L. N. Feldborg, M. Linares, M. Paradinás, S. Stafström, C. Ocal, B. Nieto-Ortega, J. Casado, J. T. López Navarrete, R. Lazzaroni, S. D. Feyter, D. B. Amabilino, *J. Am. Chem. Soc.* **2010**, *132*, 9350–9362; c) T. Ogoshi, M. Hashizume, T.-a. Yamagishi, Y. Nakamoto, *Langmuir* **2010**, *26*, 3169–3173.
- [11] a) G. Longhi, S. Abbate, F. Lebon, N. Castellucci, P. Sabatino, C. Tomasini, *J. Org. Chem.* **2012**, *77*, 6033–6042; b) V. Setnička, J. Nový, S. Böhm, N. Sreenivasachary, M. Urbanová, K. Volka, *Langmuir* **2008**, *24*, 7520–7527; c) M. Urbanová, *Chirality* **2009**, *21*, E215–E230.

Received: August 6, 2013

Published online: October 29, 2013